Orbital: The Electronic Journal of Chemistry
journal homepage: www.orbital.ufms.br
ISSN 1984-6428

| Vol 9 | | No. 4 | | July-September 2017 |

Full Paper

Montmorillonite K-10 Supported 11-molybdo-1-vanadophosphoric Acid ($H_4PMo_{11}V_1O_{40}$/K-10) Catalysts for Environmentally Benign Synthesis of 2*H*-indazolo[2,1-b]phthalazine-triones Under Solvent-free Condition

Laxmikant D. Chavan[a], Bhagwat B. Nagolkar[b], Trimbak K. Chondhekar[b], Sunil G. Shankarwar[b]*

[a]*Department of Chemistry, Jawaharlal Nehru Engineering College, Aurangabad- 431 003, M.S., India.*
[b]*Department of Chemistry, Dr. Babasaheb Ambedkar Marathwada University, Aurangabad – 431 004, M.S., India.*

Article history: Received: 09 June 2016; revised: 22 October 2016; accepted: 27 July 2017. Available online: 24 September 2017. DOI: http://dx.doi.org/10.17807/orbital.v9i4.873

Abstract: A series of 11-molybdo-1-vanadophosphoric acid supported on montmorillonite K-10 catalysts were prepared and characterized by FT-IR spectroscopy, thermal analysis, XRD, BET and SEM analysis techniques. Characterization data reveals the chemical immobilization of $H_4PMo_{11}V_1O_{40}$ catalyst on the montmorillonite K-10 support. The catalytic performance of synthesized catalysts was investigated for the synthesis of 2H-indazolo[2,1-b]phthalazine-1,6,11(13*H*)-trione derivatives by one-pot three-component reaction of phthalhydrazide, dimedone and aromatic aldehydes under solvent-free conditions. Among different catalysts, 20% $H_4PMo_{11}V_1O_{40}$ supported on to montmorillonite K-10 showed the highest catalytic activity. Effect of reaction parameters such as catalyst loading, temperature and the nature of substituents on the aromatic ring of aldehydes were also evaluated. The protocol developed using $H_4PMo_{11}V_1O_{40}$/K-10 has several distinct advantages such as operational simplicity, short reaction time, high yield, reusable catalyst and preclusion of toxic solvent.

Keywords: 2*H*-indazolo[2,1-b]phthalazine-triones; supported heteropoly acids; montmorillonite K-10 clay; solvent-free condition

1. INTRODUCTION

Heteropoly acids (HPAs) have attracted increasing interest in recent time for their intrinsic multi-functionality, high acidic strength and tunable redox properties in the field of catalysis [1]. Among various heteropoly acids, Keggin-type HPAs have been widely used as homogeneous and heterogeneous catalyst for acid-base and oxidation reactions, because of their very strong Bronsted acidity and high thermal stability [2,3]. The Keggin-type HPAs are typically represented by the general formula H_{8-x} $[XM_{12}O_{40}]$, where X is the hetero atom (usually P^{5+} or Si^{4+}), x is it's oxidation state and M is its addenda atom (most frequently W^{6+} or Mo^{6+}). The M^{6+} ions can be substituted by many other metal ions, e.g., V^{5+}, Co^{2+}, Zn^{2+} etc [4]. The effect of vanadium (V) substitution for molybdenum (VI) in molybdophosphoric acid has already been the subject of studies in the literature [5]. The HPAs has several advantages such as non-corrosive nature, strong Bronsted acidity, multifuctionality, structural mobility, reusability, non-toxicity and experimental simplicity [6]. But, the main drawback of HPAs as catalysts is that their low surface area (<10m^2/g) and separation problem from reaction mixture, which hinders its practical utilization as a solid acid [7]. To overcome the above described problems, HPAs have been supported on various acidic or neutral supports such as SiO_2[8], TiO_2[9], ZrO_2,[10], activated carbon [11] or clay[12]. Among them, montmorillonite clay has attracted much attention as supporting material because of its relatively high thermal stability, high surface area, environmental compatibility, low cost, operational simplicity and unique textural property [13].

Heterocyclic compounds containing phthalazine moiety have attracted considerable

*Corresponding author. E-mail: shankarwar_chem@yahoo.com

attention in recent years owing to their pharmacological and biological activities [14] such as anticonvulsant [15], cardiotonic [16] and vasorelaxant activities [17]. In addition, they also act as potent inhibitors of vascular endothelial growth factor receptor II (VEGFR-2) [18] and show promising properties as new luminescence materials or fluorescence probes [19]. There are several reports in the literature for the synthesis of 2H-indazolo[2,1-b]phthalazine-trione derivatives employing aromatic aldehydes, cyclic 1,3-diketones and phthalhydrazide, utilizing different types of catalysts such as silica supported polyphosphoric acid [20], H_2SO_4 in H_2O-EtOH or ionic liquid [21], p-TSA [22], $Mg(HSO_4)_2$ [23], $Ce(SO_4)_2.4H_2O$ [24], TMSCl [25], alum [26], [BMIm]Br [27], silica supported $KHSO_4$ [28], $H_{14}[NaP_5W_{30}O_{110}]/SiO_2$ [29] and CuO-ZnO nanocatalyst [30]. Each of these methods have their own advantages but also suffer from one or more disadvantages such as prolonged reaction time, use of toxic organic solvents, tedious work-up processes, harsh reaction conditions and low yield of products. Thus, it is important to introduce efficient synthetic routes for the synthesis of 2*H*-indazolo[2,1-b]phthalazine-1,6,11(13*H*)-trione derivatives.

The present work deals with the preparation of a series of 11-molybdo-1-vanadophosphoric acid supported on montmorillonite K-10 catalysts and its characterization by FT-IR spectroscopy, thermal analysis, XRD, BET and SEM analysis techniques. These catalyst were used for the synthesis of 2*H*-indazolo[2,1-b]phthalazine-1,6,11(13*H*)-trione derivatives by one-pot three-component reaction of phthalhydrazide, dimedone and aromatic aldehydes under solvent-free conditions.

2. MATERIAL AND METHODS

2.1 Catalyst Preparation

2.1.1. Preparation of 10-molybdo-2-vanadophosphoric acid, $H_4PMo_{11}V_1O_{40}$

$H_4PMo_{11}V_1O_{40}$ catalyst was prepared according to the reported procedure [31]. Na_2HPO_4 (7.1 g, 0.050 mol) was dissolved in water (100 mL) and mixed with sodium metavanadate (6.1 g, 0.050 mol) that had been dissolved by boiling in water (100 mL). The mixture was cooled and acidified to a red colour with concentrated sulphuric acid (5 mL). To this mixture was added a solution of Na_2MoO_4. $2H_2O$ (133 g, 0.55 mol) dissolved in water (200 mL). Finally, concentrated sulphuric acid (85 mL) was added slowly with vigorous stirring of the solution. With this addition, the dark red colour changed to lighter red. The heteropoly acid was then extracted with diethyl ether (400 mL) after the water solution was cooled. In this extraction, the heteropoly etherate was present in the middle layer; the aqueous layer (bottom) was yellow and probably contained vanadyl species. After separation, a stream of air was passed through the heteropoly etherate layer to free it of diethyl ether. The orange solid that remained was dissolved in water (50 mL), concentrated to the first appearance of crystals in a vacuum desiccator over concentrated sulphuric acid, and then allowed to crystallize further. The orange crystals that formed were filtered, washed with water, and air-dried (28 g, 23%). The amount of water of crystallization varied slightly from sample to sample.

2.1.2. Preparation of montmorillonite K-10 supported 11-molybdo-1-vanadophosphoric acid, $H_4PMo_{11}V_1O_{40}$/K-10

A series of catalysts having 10, 20, and 30% loading of $H_4PMo_{11}V_1O_{40}$ on to montmorillonite K-10 clay were synthesized by means of incipient wetness impregnation method [32]. For preparation of $H_4PMo_{11}V_1O_{40}$/K-10, montmorillonite K-10 clay was dried in an oven to 120 °C for 1 h prior to its use as support. To prepare the catalyst with 10, 20 and 30% of $H_4PMo_{11}V_1O_{40}$ loading on to the montmorillonite K-10 support, the appropriate amounts of $H_4PMo_{11}V_1O_{40}$ was dissolved in 8 mL of dry methanol and the hot support was added to the solution under constant stirring with a glass rod. The slurry was stirred vigorously and air-dried. Finally, the resulting material was dried in oven at 120 °C for 2 h and subsequently calcined at 285 °C for 3h.

2.2. Characterization techniques

FT-IR spectra were recorded with KBr pellets using a Bruker, Germany (Model 3000 hyperion microscope with vertex 80 FTIR system) spectrometer. Powder X-ray diffraction (XRD) measurements were obtained with a Philips X'pert MPD System instrument using Cu Kα radiation. The FE-SEM was performed with a JSM-7600F microscope operated at 30 kV. The TG-DTA measurements of the samples were carried out using Thermal Analyzer (Perkin Elmer, Model Diamond TG-DTA) with about 10 mg of sample in a platinum crucible at a heating rate of 10 °C min^{-1} in an air atmosphere. The specific surface areas of the support and catalysts were determined by BET method

on a Micromeritics ASAP 2010 apparatus at a liquid nitrogen temperature with N_2 as the absorbent at -196 °C. ^{1}H NMR spectra were recorded on a Bruker Avance III HD-300 spectrometer and ^{13}C NMR was recorded on a Bruker DRX-300 spectrometer using TMS as an internal reference. Mass spectra were recorded on Waters UPLC-TQD Mass spectrometer using electrospray ionization technique. The uncorrected melting points of compounds were taken in an open capillary in a paraffin bath.

2.3. General procedure for the preparation of 2*H*-indazolo[2,1-b]phthalazine-1,6,11(13*H*)-trione derivatives using montmorillonite K-10 supported $H_4PMo_{11}V_1O_{40}$ as a catalyst

A mixture of dimedone (1 mmol), phthalhydrazide (1 mmol), aromatic aldehyde (1.1 mmol) and 20% $H_4PMo_{11}V_1O_{40}$/K-10 (0.15 g) was rapidly stirred and heated at 100 °C for the appropriate time. Progress of the reaction was monitored by TLC. After reaction completion, the reaction mixture was cooled to room temperature and dichloromethane (20 mL) was added. The catalyst was recovered from residue. The filtrate was concentrated under vacuum to afford crude product. The pure product was obtained by further recrystalization in aqueous ethanol (25%). Recovered catalyst was washed with dichloromethane (10 mL) and calcined at 150 °C for 2 h, before reusing. All the products are known compounds. Their melting points are compared with reported values in literature (given in Table 4). The spectral data (^{1}H NMR, ^{13}C NMR and Mass spectroscopy) of some selected 2*H*-indazolo[2,1-b]phthalazine-1,6,11(13*H*)-triones are given below.

2.3.1. Spectral data for selected 2*H*-indazolo[2,1-b]phthalazine-1,6,11(13*H*)-triones

3,3-Dimethyl-13-phenyl-3,4-dihydro-2*H*-indazolo[1,2-b]phthalazine-1,6,11(13*H*)-trione (**4a**): Yellow powder; ^{1}H NMR ($CDCl_3$, 300 MHz): δ = 1.20 (s, 6H), 2.32 (s, 2H), 3.20-3.26 (d, J = 18 Hz, 1H), 3.38-3.44 (d, J = 18 Hz, 1H), 6.43 (s, 1H), 7.23-7.35 (m, 3H), 7.38-7.42 (m, 2H), 7.79-7.85 (m, 2H), 8.22-8.36 (m, 2H); ^{13}C NMR: ($CDCl_3$, 75 MHz): δ = 28.60, 28.84, 34.79, 38.20, 51.10, 65.10, 118.74, 127.28, 127.85, 128.10, 128.84, 129.13, 129.24, 133.65, 134.63, 136.57, 150.99, 154.42, 156.17, 192.22; EI-MS: *m/z* (%) = 373 $(M+H)^+$.

3,3-Dimethyl-13-(4-fluorophenyl)-3,4-dihydro-2*H*-indazolo[1,2-b]phthalazine-1,6,11(13*H*)-trione (**4j**): Yellow powder; ^{1}H NMR ($CDCl_3$, 300 MHz): δ = 1.20 (s, 6H), 2.33 (s, 2H), 3.20-3.26 (d, J = 18 Hz, 1H), 3.37-3.43 (d, J = 18 Hz, 1H), 6.42 (s, 1H), 6.96-7.04 (m, 2H), 7.36-7.43 (m, 2H), 7.80-7.86 (m, 2H), 8.22-8.36 (m, 2H); ^{13}C NMR: ($CDCl_3$, 75 MHz): δ = 28.58, 28.82, 34.78, 38.17, 51.06, 64.41, 115.68, 115.97, 118.33, 127.81, 128.14, 129.09, 129.12, 129.20, 132.41, 132.45, 133.70, 134.74, 151.15, 154.51, 156.13, 161.19, 164.46, 192.25; EI-MS: *m/z* (%) = 391 $(M+H)^+$.

3,3-Dimethyl-13-(4-nitrophenyl)-3,4-dihydro-2*H*-indazolo[1,2-b]phthalazine-1,6,11(13*H*)-trione (**4g**): Yellow powder; ^{1}H NMR ($CDCl_3$, 300 MHz): δ = 1.21 (s, 6H), 2.33 (s, 2H), 3.22-3.28 (d, J = 18 Hz, 1H), 3.38-3.44 (d, J = 18 Hz, 1H), 6.49 (s, 1H), 7.59-7.62 (d, J = 9 Hz, 2H), 7.84-7.90 (m, 2H), 8.15-8.18 (d, J = 9 Hz, 2H), 8.22-8.38 (m, 2H); ^{13}C NMR: ($CDCl_3$, 75 MHz): δ = 28.44, 28.77, 34.80, 38.12, 50.90, 64.24, 114.57, 117.35, 123.46, 124.08, 127.79, 128.19, 128.30, 128.70, 129.04, 129.44, 134.03, 134.03, 134.87, 143.61, 147.94, 151.81, 154.65, 156.01, 163.09, 192.12; EI-MS: *m/z* (%) = 418 $(M+H)^+$.

3. RESULTS AND DISCUSSION

3.1. Characterization of the catalysts

3.1.1. FT-IR analysis

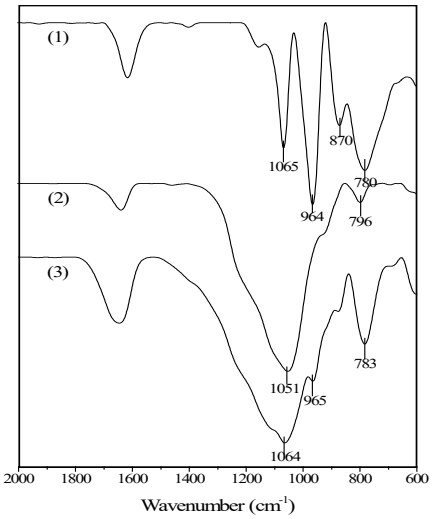

Figure 1. FT-IR spectra of the bulk $H_4PMo_{11}V_1O_{40}$ (1), montmorillonite K-10 (2) and 20% $H_4PMo_{11}V_1O_{40}$/K-10 (3).

Chemical immobilization of $H_4PMo_{11}V_1O_{40}$ on the montmorillonite K-10 support was confirmed by

FT-IR analysis. FT-IR spectra of the bulk $H_4PMo_{11}V_1O_{40}$, montmorillonite K-10 clay and 20% $H_4PMo_{11}V_1O_{40}$/K-10 are shown in Figure 1. The primary structure of $H_4PMo_{11}V_1O_{40}$ was confirmed by four characteristic FT-IR bands located between 800 and 1100 cm^{-1} [33]. The main characteristic FT-IR bands of $H_4PMo_{11}V_1O_{40}$ are observed at 1065 (P-O stretching), 964 (M=O stretching), 870 (inter-octahedral M-O-M stretching) and 780 cm^{-1} (intra-octahedral M-O-M stretching). Upon being supported on montmorillonite K-10, some of the characteristic FT-IR bands were appeared at 1064 (P-O stretching), 965 (M=O stretching), 783 cm^{-1} (intra-octahedral M-O-M stretching) and other bands were merged in with the montmorillonite K-10 bands. In other words, the characteristic FT-IR bands of $H_4PMo_{11}V_1O_{40}$ in the 20% $H_4PMo_{11}V_1O_{40}$/K-10 were observed at slightly shifted positions compared to those of bulk $H_4PMo_{11}V_1O_{40}$. This might be due to strong chemical interaction between two components. Thus, it can be established that FT-IR spectroscopy can partially prove the immobilization of $H_4PMo_{11}V_1O_{40}$ on the montmorillonite K-10 support.

3.1.2. Thermal Analysis

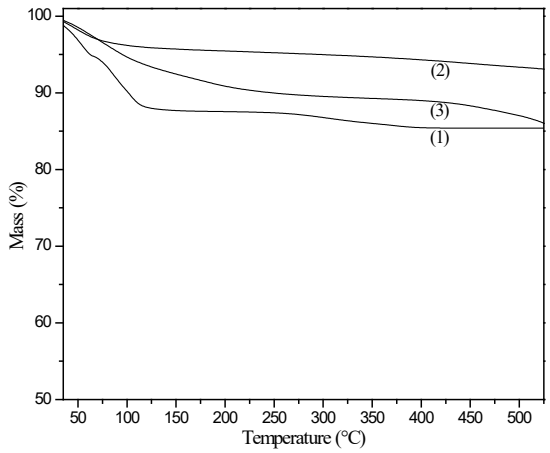

Figure 2. Thermal analysis of the bulk $H_4PMo_{11}V_1O_{40}$ (1), montmorillonite K-10 (2) and 20% $H_4PMo_{11}V_1O_{40}$/K-10 (3).

The thermal stability of the bulk $H_4PMo_{11}V_1O_{40}$, montmorillonite K-10 and 20% $H_4PMo_{11}V_1O_{40}$/K-10 was examined by TGA analysis and the TGA graphs are depicted in Figure 2. The initial weight loss of about 11.6% in the TGA data of $H_4PMo_{11}V_1O_{40}$ up to a temperature of 120 °C corresponds to the loss of free and adsorbed water. A gradual mass loss of about 2.7% up to 500 °C, which was attributed to the removal of more hydrated or structural water. The TGA data of montmorillonite K-10 showed a mass loss of about 4% up to a temperature 120 °C corresponds to dehydration of surface adsorbed water. A gradual mass loss of about 2.5% up to a temperature 500 °C, which was caused due to dehydration of interlayer water. The TGA of 20% $H_4PMo_{11}V_1O_{40}$/K-10 showed about 10.2% mass loss up to a temperature 275 °C, which was attributed to the loss of adsorbed water molecules. A gradual mass loss of about 2.6% up to 500 °C, which was caused due to release of more hydrated or structural water. These results indicate that the thermal stability of $H_4PMo_{11}V_1O_{40}$ was increased after being supported on to the montmorillonite K-10 support. This increase in thermal stability might be due to the formation of intermolecular bonding between the montmorillonite K-10 support and $H_4PMo_{11}V_1O_{40}$ and indicated the presence of chemical interaction between them.

3.1.3. FE-SEM Analysis

Field emission scanning electron micrographs of montmorillonite K-10 and 20% $H_4PMo_{11}V_1O_{40}$/K-10 catalyst are shown in Figure 3. These images clearly show the surface morphology of the 20% $H_4PMo_{11}V_1O_{40}$/K-10 catalyst was different to that of the montmorillonite K-10 support, as can be seen from the Figure 3 (a) and Figure 3 (b). This result indicates that surface morphology of montmorillonite K-10 was altered due to the dispersion and insertion of catalyst over the surface of support.

3.1.4. BET Surface area and total pore volume

The BET surface area and total pore volume of $H_4PMo_{11}V_1O_{40}$, montmorillonite K-10 and 20% $H_4PMo_{11}V_1O_{40}$/K-10 catalyst are presented in Table 1. It is interesting to mention here that surface area and total pore volume of 20% $H_4PMo_{11}V_1O_{40}$/K-10 catalyst diminish with respect to the montmorillonite K-10 support. The decrease in surface area and pore volume may be attributed to the blockage of pores by $H_4PMo_{11}V_1O_{40}$.

Table 1. Surface properties of $H_4PMo_{11}V_1O_{40}$, Montmorillonite K-10 and 20% $H_4PMo_{11}V_1O_{40}$/K-10 catalyst.

Sample	BET surface area (m^2/g)	Total pore volume (cm^3/g)
$H_4PMo_{11}V_1O_{40}$	10.46	0.01
Montmorillonite K-10	242.01	0.35
20% $H_4PMo_{11}V_1O_{40}$/K-10	85.97	0.18

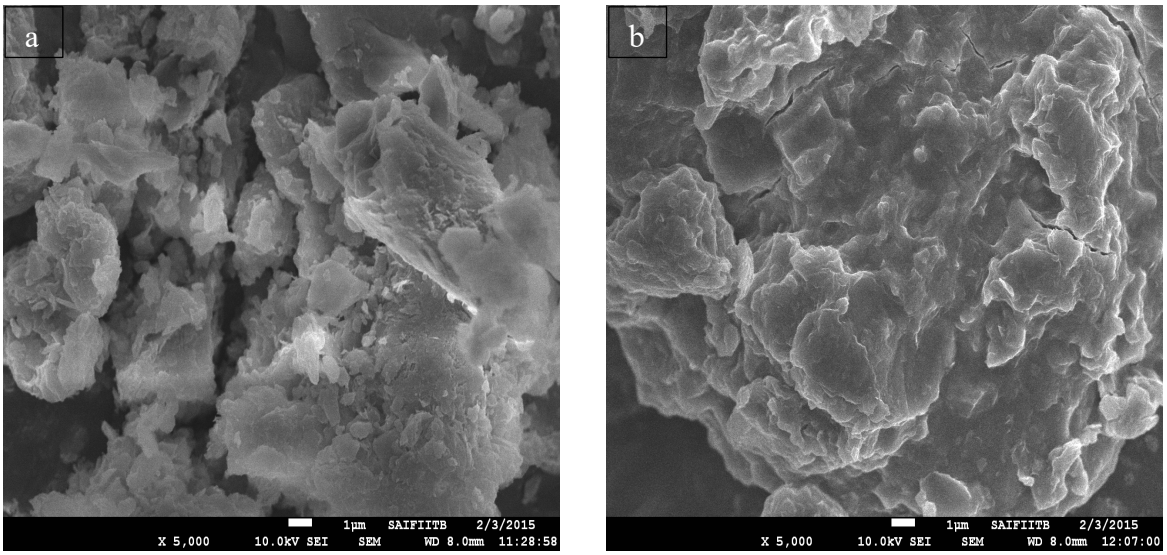

Figure 3. FE-SEM images of the montmorillonite K-10 (a) and 20% $H_4PMo_{11}V_1O_{40}$/K-10 (b).

3.1.5. Powder XRD analysis

The XRD patterns of $H_4PMo_{11}V_1O_{40}$, montmorillonite K-10 and 20% $H_4PMo_{11}V_1O_{40}$/K-10 catalyst are shown in Figure 4. The XRD pattern of $H_4PMo_{11}V_1O_{40}$ showed four intense peaks with 2θ values of 7.35, 8.14, 9.03 and 29.08, which corresponded to basal d-spacing (d_{001}) values of about 12.01, 10.85, 9.78 and 3.07 nm. Several other peaks were also observed which demonstrates that $H_4PMo_{11}V_1O_{40}$ was crystalline in nature. On the other hand, montmorillonite K-10 showed three intense peaks with 2θ values of 8.98, 19.96 and 26.77 corresponding to the basal d-spacing (d_{001}) values 9.84, 4.44 and 3.32 nm. Several other peaks were also observed which indicated that montmorillonite K-10 was nano-crystalline in nature. It is noteworthy that 20% $H_4PMo_{11}V_1O_{40}$/K-10 catalyst exhibited no characteristic peaks of $H_4PMo_{11}V_1O_{40}$ but showed almost similar peaks that those observed in diffractogram of montmorillonite K-10, indicating the retention of the original characteristics of montmorillonite K-10.

3.2. Catalytic activity

To choose optimum conditions, first, the effect of catalyst composition on the rate of the reaction was evaluated for the synthesis of 2*H*-indazolo[2,1-b]phthalazine-1,6,11(13*H*)-trione by one-pot three-component reaction of phthalhydrazide, dimedone and benzaldehyde in presence of various amounts of $H_4PMo_{11}V_1O_{40}$/K-10 catalyst under solvent-free conditions and the results are summarized in Table 2. It can be seen from Table 2, pure montmorillonite K-10 has shown moderate catalytic activity in terms of reaction time and yield of products. Increasing the loading of $H_4PMo_{11}V_1O_{40}$ from 10% to 20% on montmorillonite K-10 support, the conversion increases and require short reaction time, but thereafter, it was not increased on further loading to 30% $H_4PMo_{11}V_1O_{40}$ on montmorillonite K-10 support. It is interesting to note that the activity of bulk $H_4PMo_{11}V_1O_{40}$ is significantly lower than that of the same amount supported on montmorillonite K-10 support. The enhanced catalytic activity of 20% $H_4PMo_{11}V_1O_{40}$/K-10 may be due to a high dispersion of the $H_4PMo_{11}V_1O_{40}$ on montmorillonite K-10 support, providing more surface area and availability of more number of active sites than bulk $H_4PMo_{11}V_1O_{40}$. So, 20% $H_4PMo_{11}V_1O_{40}$/K-10 (1.5 g) catalyst was found to be optimal quantity and sufficient to push the reaction forward.

Table 2. Effect of various $H_4PMo_{11}V_1O_{40}$ loadings on the efficiency of $H_4PMo_{11}V_1O_{40}$/K-10 catalyst.

Entry	Catalyst	Time (min)	Yield (%)[a]
01	$H_4[PMo_{11}V_1O_{40}]$ $30H_2O$	35	79
02	Montmorillonite K-10	60	65
03	10% $H_4PMo_{11}V_1O_{40}$ / K-10	30	86
04	20% $H_4PMo_{11}V_1O_{40}$ / K-10	20	95
05	30% $H_4PMo_{11}V_1O_{40}$ / K-10	20	95

Reaction conditions: dimedone (1 mmol), phthalhydrazide (1 mmol), benzaldehyde (1.1 mmol) and $H_4PMo_{11}V_1O_{40}$/K-10 (0.15 g) at 100 °C under solvent-free conditions. [a]Isolated yield.

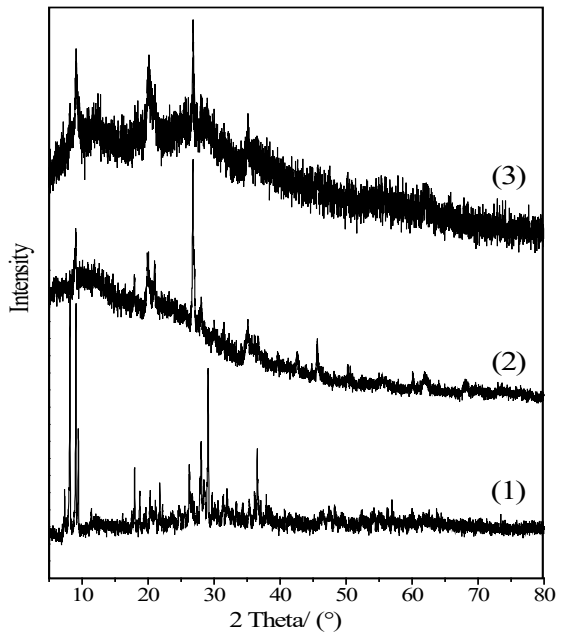

Figure 4. XRD patterns of bulk $H_4PMo_{11}V_1O_{40}$ (1), montmorillonite K-10 (2) and 20% $H_4PMo_{11}V_1O_{40}$/K-10 (3).

Next, for optimization of reaction temperature, the reaction was carried out at different temperatures under solvent-free condition. The results are shown in Table 3. As it is shown in Table 3, higher yield of product was obtained at 100 °C in shorter reaction time. The yield of product and reaction time show no appreciable change with further rise in reaction temperature.

Table 3. Effect of reaction temperature.

Entry	Temperature (°C)	Time (min)	Yield (%) [a]
01	80 °C	40	88
02	90 °C	28	90
03	100 °C	20	95
04	110 °C	20	95
05	120 °C	20	95

Reaction conditions: dimedone (1 mmol), phthalhydrazide (1 mmol), benzaldehyde (1.1 mmol) and $H_4PMo_{11}V_1O_{40}$/K-10 (0.15 g) under solvent-free conditions. [a]Isolated yield.

After optimizing the conditions, the generality of this method was examined by the reaction of dimedone and phthalhydrazide with various aromatic aldehydes carrying either electron-releasing or electron-withdrawing groups in presence of 20% $H_4PMo_{11}V_1O_{40}$/K-10 (0.15 g) at 100 °C under solvent-free condition and the results are shown in Table 4. In all cases, aromatic aldehydes carrying either electron-releasing or electron-withdrawing groups reacted successfully and gave the products in high yields.

Table 4. Synthesis of 2H-indazolo[2,1-b]phthalazine-trione derivatives using 20% $H_4PMo_{11}V_1O_{40}$/K-10 as catalyst.

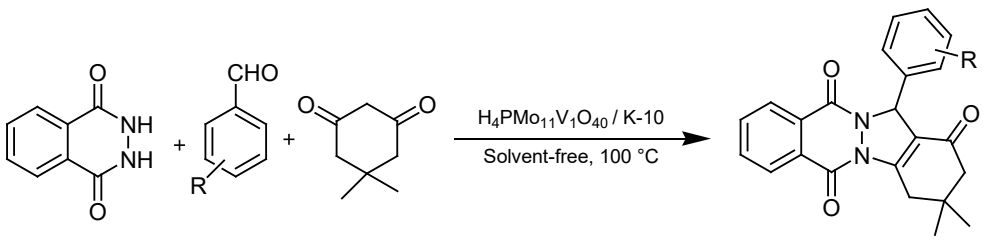

Entry	Aldehyde	Product	Time (min)	Isolated Yield (%)[a]	Melting point (°C) Found	Melting point (°C) Reported	Reference
1	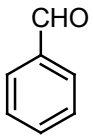	**4a**	20	95	204-205	204-206	22
2	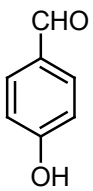	**4b**	26	96	222-224	225-227	28

3	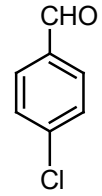	**4c**	16	94	259-261	262-264	22
4	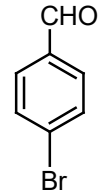	**4d**	20	98	262-264	265-267	22
5	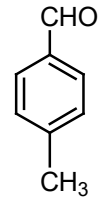	**4e**	24	95	226-228	227-229	35
6	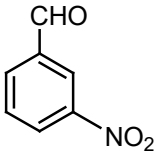	**4f**	22	89	271-273	270-272	35
7	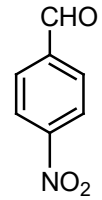	**4g**	25	90	214-216	217-219	20
8	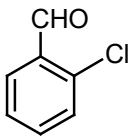	**4h**	15	98	260-262	264-266	22
9	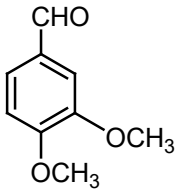	**4i**	35	88	185-187	185-186	34
10	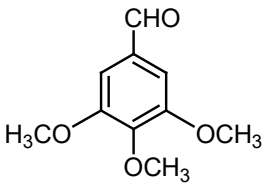	**4j**	38	86	231-233	232-234	20
11	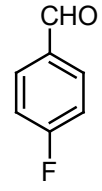	**4k**	18	94	214-216	217-219	22
12	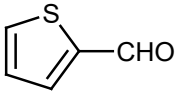	**4l**	32	86	217-219	219-221	28

Reaction conditions: dimedone (1 mmol), phthalhydrazide (1 mmol), aromatic aldehyde 4a-l (1.1 mmol) and 20% $H_4PMo_{11}V_1O_{40}$/K-10 (0.15 g) at 100 °C under solvent-free conditions. [a]Isolated yield.

3.3. Recyclability of the catalyst

In order to regenerate a 20% $H_4PMo_{11}V_1O_{40}$/K-10 catalyst from the reaction mixture upon completion of the reaction, the catalyst was separated by simple filtration process. The recovered catalyst was washed with dichloromethane for several times followed by drying at 120 °C in an air oven. The results of a reusability study show that the catalyst could be reused at least three times with only a slight reduction in its catalytic activity i.e. the conversion of 95% in the first run decreases to about 89% in the second run and to 82% in the third run. This decrease in catalytic activity may be due to the leaching of catalyst from the clay support.

4. CONCLUSION

A series of 11-molybdo-1-vanadophosphoric acid supported on montmorillonite K-10 catalysts were prepared and their catalytic performance was investigated for the synthesis of 2H-indazolo[2,1-b]phthalazine-1,6,11(13H)-trione derivatives. FT-IR analysis results indicate that the $H_4PMo_{11}V_1O_{40}$ was chemically immobilized on the montmorillonite K-10 support. The XRD, BET and FE-SEM results revealed that $H_4PMo_{11}V_1O_{40}$ was finely dispersed on montmorillonite K-10 support. In the model one-pot three-component reaction of phthalhydrazide, dimedone and benzaldehyde, the 20% $H_4PMo_{11}V_1O_{40}$ loaded on montmorillonite K-10 catalyst showed the highest efficacy compared to the bulk $H_4PMo_{11}V_1O_{40}$ catalyst, as well as (10% and 30%) $H_4PMo_{11}V_1O_{40}$ loaded on montmorillonite K-10 catalysts. The high catalytic activity of 20% $H_4PMo_{11}V_1O_{40}$/K-10 catalyst was attributed to the high surface area and large number of Bronsted acid sites. Thus, the 20% $H_4PMo_{11}V_1O_{40}$/K-10 catalyst is thermally stable, environmentally benign, easy and inexpensive to make, as well as it can be easily separated from the reaction mixtures and reused several times. Moreover, the protocol developed using 20% $H_4PMo_{11}V_1O_{40}$/K-10 is advantageous in terms of simple experimentation, short reaction times, high yields of the products and preclusion of toxic solvents.

5. ACKNOWLEDMENTS

The authors are thankful to the Head, Department of Chemistry, Dr. Babasaheb Ambedkar Marathwada University, Aurangabad and Principal, Jawaharlal Nehru Engineering College, Aurangabad-431 004 (MS), India for providing the laboratory facility.

6. REFERENCES AND NOTES

[1] Mizuno, N.; Misono, M. *Chem. Rev.* **1998,** *98*, 199. [CrossRef]

[2] Hill, C. L.; Prosser-McCartha, C. M. *Coord. Chem. Rev*. **1995**, *143*, 407. [CrossRef]

[3] Okuhara, T.; Mizuno, N.; Misono, M. *Adv. Catal.* **1996**, *41*, 113. [CrossRef]

[4] Kozhevnikov, I. V. *Chem. Rev*. **1998**, *98*, 171. [CrossRef]

[5] Khenkin, A.; Neumann, R.; Sorokin, A.; Tuel, A. *Catal. Lett*. **1999**, *63*, 189. [CrossRef]

[6] Bhorodwaj, S. K.; Dutta, D. K. *Appl. Clay Sci*. **2011**, *53*, 347. [CrossRef]

[7] Hong, U. G.; Park, D. R.; Park, S.; Seo, J. G.; Bang, Y.; Hwang, S.; Youn, M. H.; Song, I. K. *Catal. Lett.* **2009**, *132*, 377. [CrossRef]

[8] Esfahani, M. N.; Montazerozohari, M.; Gholampour, T. *Bull. Korean Chem. Soc.* **2010**, *31*, 3653. [CrossRef]

[9] Carriazo, D.; Addamo, M.; Marci, G.; Martin, C.; Palmisano, L.; Rives, V. *Appl. Catal. A: Gen*. **2009**, *356*, 172. [CrossRef]

[10] Devassy, B. M.; Halligudi, S. B. *J. Catal.* **2005**, *236*, 313. [CrossRef]

[11] Rafiee, E.; Zolfagharifar, Z.; Joshaghani, M.; Eavani, S. *Synth. Commun*. **2011**, 41, 459. [CrossRef]

[12] Yadav, G. D.; Deshmukh, S. A.; Asthana, N. S. *Ind. Eng. Chem. Res.* **2005**, *44*, 7969. [CrossRef]

[13] Bhorodwaj, S. K.; Pathak, M. G.; Dutta, D. K. *Catal. Lett.* **2009**, *133*, 185. [CrossRef]

[14] Carling, R. W.; Moore, K. W.; Street, L. J.; Wild, D.; Isted, C.; Leeson, P. D.; Thomas, S.; O'Conner, D.; McKernan, R. M.; Quirk, K.; Cook, S. M.; Atack, J. R.; Wafford, K. A.; Thompson, S. A.; Dawson, G. R.; Ferris, P.; Castro, J. L. *J. Med. Chem*. **2004**, *47*, 1807. [CrossRef]

[15] Nomoto, Y.; Obase, H.; Takai, H.; Teranishi, M.; Nakamura, J.; Kubo, K. *Chem. Pharm. Bull*. **1990**, *38*, 2179. [CrossRef]

[16] Watanabe, K.; Kabasawa, Y.; Takase, Y.; Matsukura, M.; Miyazaki, K.; Ishihara, H.; Kodama, K.; Adachi, H. *J. Med. Chem.* **1998**, *41*, 3367. [CrossRef]

[17] Potts, K. T.; Lovelette, C. *J. Org. Chem.* **1969**, *34*, 3221. [CrossRef]

[18] Piatnitski, E. L.; Duncton, M. A. J.; Kiselyov, A. S.; Katoch-Rouse, R.; Sherman, D.; Milligan, D. L.; Balagtas, C.; Wong, W. C.; Kawakami, J.; Doody, J. F. *Bioorg. Med. Chem. Lett*. **2005**, *15*, 4696. [CrossRef]

[19] Wu, H.; Chen, X. M.; Wan, Y.; Xin, H. Q.; Xu, H. H.; Ma, R.; Yue, C. H.; Pang, L. L. *Lett. Org. Chem.* **2009**, *6*, 219. [CrossRef]

[20] Shaterian, H. A.; Hosseinian, A.; Ghashanh, M. *Arkivoc* **2009**, *2*, 59.

[21] Khurana, J. M.; Magoo, D. *Tetrahedron Lett*. **2009**, *50*, 7300. [CrossRef]

[22] Sayyafi, M.; Seyyedhamzeh, M.; Khavasi, H. R.; Bazgir, A. *Tetrahedron* **2008**, *64*, 2375. [CrossRef]

[23] Shaterian, H. R.; Khorami, F.; Amirzadeh, A.;

Doostmohammadi, R.; Ghashang, M. *J. Iran Chem. Res*. **2009**, *2*, 57.

[24] Mosaddegh, E.; Hassankhani, A. *Tetrahedron Lett.* **2011**, *52*, 488. [CrossRef]

[25] Nagarapu, L.; Bantu, R.; Mereyala, H. B. *J. Heterocycl. Chem.* **2009**, *46*, 728. [CrossRef]

[26] Madje, B. R.; Bharad, J. V.; Ubale, M. B.; Shingare, M. S. *Orbital: Electron. J. Chem.* **2012**, *4*, 202.

[27] Shekouhy, M.; Hasaninejad, A. *Ultrason. Sonochem*. **2012**, *19*, 307. [CrossRef]

[28] Raghuvanshi, D. S.; Kumari, K.; Allam, B. K.; Singh, K. N. *Ind. J. Chem.* **2014**, *53*, 1462.

[29] Gharib, A.; Khorasani, B. R. H.; Jahangir, M.; Hans, J. *Bulgarian Chem. Commun*. **2013**, *45*, 64.

[30] Albadi, J.; Shahriari, A.; Tajik, H. *Jordan J. Chem.* **2015**, *10*, 130.

[31] Kozhevnikov, I. V. Catalysis for Fine Chemical Synthesis, Chichester: Wiley, 2002, Vol. 2.

[32] Haber, J.; Pamin, K.; Matachowski, L.; Mucha, D. *Appl. Catal. A: Gen.* **2003**, *256*, 141. [CrossRef]

[33] Villabrille, P.; Romanelli, G.; Caceres, V. P. *Appl. Catal. A: Gen*. **2004**, *270*, 101. [CrossRef]

[34] Maleki, B.; Ashrafi, S. S. *J. Mex. Chem. Soc.* **2014**, *58*, 159.

[35] Afzalian, B.; Mague, J. T.; Mohamadi, M.; Ebrahimipour, S. Y.; Amiri, B. P.; Kermani, E. T. *Chin. J. Catal*. **2015**, *36*, 1101. [CrossRef]